Selective Fixed Filter Sub-band Active Noise Control System Based on Reference Signal Power Estimation

Shota Toyooka* and Ryo Matsuura* and Kenta Iwai† and Yoshinobu Kajikawa*
* Kansai University, Japan
E-mail: {k927766, k676743, kaji}@kansai-u.ac.jp
† Osaka Sangyo University, Japan
E-mail: iwai@ise.osaka-sandai.ac.jp

***Abstract*—This paper proposes a selective fixed filter sub-band active noise control system based on reference signal power estimation. The reference signal is decomposed into multiple, non-overlapping frequency sub-bands, and the control filter associated with the sub-band of highest acoustic power is dynamically activated. By updating the selected filter every 20 ms, the proposed system can effectively track rapid spectral variations in the unwanted acoustic noise. Numerical experiments using measured impulse responses demonstrate broadband noise attenuation exceeding 20 dB, even under rapidly changing noise conditions.**

I. Introduction

Active noise control (ANC) [1]–[4] is widely recognized as an effective solution for suppressing low-frequency noise, whose adverse impact on comfort and health has drawn increasing attention in recent years. ANC attenuates the unwanted acoustic noise by radiating an anti-noise signal with the same amplitude and opposite phase, thereby achieving destructive interference at the listener's ear.

Two canonical ANC architectures exist: feedforward (FF) and feedback (FB) control. FF systems can cancel broadband, stochastic noise, whereas FB systems are well suited to narrowband or periodic noise. This study focuses on FFANC systems.

In a typical FFANC system, a reference microphone captures the unwanted noise while an error microphone measures the residual error at the control point. The adaptive algorithm, represented by filtered-x normalized least-mean-squares (FxNLMS) [5]–[7], updates the control filter coefficients to minimize the residual power. However, these adaptive approaches suffer from two key limitations: (i) the filter convergence speed may be insufficient when the noise spectrum varies abruptly, and (ii) an error microphone must reside at the intended zone of quiet (ZoQ) [8]–[10]. Because the ZoQ radius shrinks with increasing frequency, placing a sensor at the eardrum, where cancellation is perceptually most relevant, is impractical; users may therefore perceive limited benefit.

A fixed-filter ANC system [11] has been introduced to alleviate the convergence and ZoQ-size limitations. In this system, error microphones are temporarily installed at the desired locations during an off-line calibration stage, and the optimal control filter is designed. During operation the pre-designed filter is applied without further adaptation, eliminating convergence issues and removing the need for an error microphone. However, fixed-filter ANC systems are highly sensitive to spectral changes in the noise source, and their performance can degrade severely under non-stationary conditions.

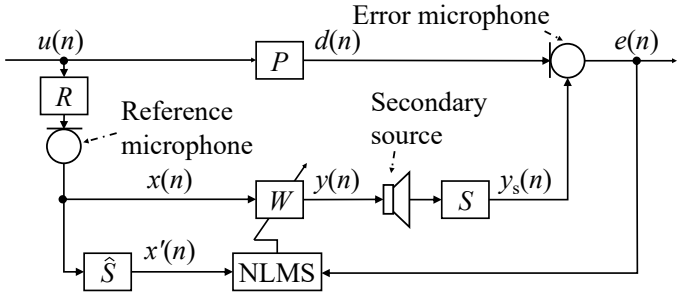

Fig. 1: Block diagram of the feedforward ANC system.

To improve robustness, the selective fixed-filter ANC (SFANC) systems [12]–[18] have been developed. These systems employ machine-learning techniques–typically a convolutional neural network (CNN)–to classify the reference signal and select an appropriate filter from a pre-designed set. Although effective, this approach increases implementation costs and risks performance degradation if the classifier makes incorrect predictions. Existing attempts to mitigate misselection still rely on data-driven models, leaving the cost issue unresolved.

This paper proposes a sub-band fixed-filter ANC system that selects the control filter via real-time noise-power estimation, eliminating any reliance on machine learning. First, a delayless sub-band ANC [19]–[22] framework is employed off-line to design a set of control filters whose coefficients are immune to sub-band boundary effects. During operation, a bank of band-pass filters estimates the instantaneous power in each sub-band; the filter corresponding to the sub-band with the highest power is then activated. By selecting the fixed filter every 20 ms, the controller maintains stable, high attenuation even when the noise spectrum fluctuates rapidly, while incurring only modest computational overhead.

II. ANC system

A. Feedforward ANC system

Fig. 1 presents the block diagram of a feedforward ANC (FFANC) system. In this configuration, R denotes the reference path from the noise source to the reference microphone, P the

979-8-3315-7206-8/25/$31.00

primary path from the noise source to the error microphone, and S the secondary path from the secondary source to the error microphone. The noise control filter is represented by W, and $\hat{S}$ denotes the secondary path model estimated in advance before ANC operation.

The z-domain expression of the error signal $e(n)$, where n is the discrete-time index, is given by

$$\begin{aligned} E(z) &= P(z)U(z) + S(z)W(z)R(z)U(z) \\ &= \big[P(z) + S(z)W(z)R(z)\big]U(z), \end{aligned} \tag{1}$$

where $P(z)$, $S(z)$, $R(z)$, and $W(z)$ are the z-transforms of the corresponding impulse responses, and $U(z)$ is the z-transform of the unwanted noise $u(n)$. The noise control filter $W(z)$ is updated by the FxNLMS algorithm [5]–[7] to minimize the residual error at the error microphone position. The optimal noise control filter that minimizes the mean-squared error is

$$W^o(z) = -\frac{P(z)}{R(z)S(z)}. \tag{2}$$

The time-domain update equation of the noise control filter is

$$\mathbf{w}(n+1) = \mathbf{w}(n) - \frac{\alpha\, e(n)\, \mathbf{x}'(n)}{\|\mathbf{x}'(n)\|^2 + \beta}, \tag{3}$$

where α is the step-size parameter and β is a small positive regularization constant that prevents division by zero. Here, $\mathbf{w}(n)$ and $\mathbf{x}'(n)$ denote the vectors of the noise control filter and the filtered reference signal after filtering through the secondary path model $\hat{S}(z)$. The two vectors are defined as

$$\mathbf{w}(n) = \big[w_0(n), w_1(n), \cdots, w_{M-1}(n)\big]^\top, \tag{4}$$

$$\mathbf{x}'(n) = \big[x'(n), x'(n-1), \cdots, x'(n-M+1)\big]^\top, \tag{5}$$

where M is the filter length (number of taps) and $(\cdot)^\top$ denotes the transpose operator.

Although the FFANC system can attenuate broadband noise, the LMS adaptation used to update the control filter W often converges slowly. One remedy is the so-called fixed-filter ANC, which dispenses with online adaptation entirely. In the offline stage, error microphones are placed at the intended quiet zones and an optimal control filter $W^o(z)$ is pre-designed on the basis of the configuration in Fig. 1. During the operation, the adaptive filter W of the conventional FFANC is simply replaced by its pre-designed counterpart $W^o(z)$; consequently, no error microphones are required for residual-error acquisition, and convergence issues are eliminated. The trade-off is that the fixed-filter approach yields a nearly uniform attenuation over the full frequency range; hence, it cannot deliver pronounced suppression when the disturbance energy is concentrated in a narrow band.

B. Selective Fixed Filter ANC System

To solve the aforementioned problems, the SFANC systems [12]–[17] have been proposed. The SFANC employs a deep-learning classifier to choose, in real time, among a set of pre-designed control filters so as to suppress the incident noise. Since the control filter is selected rather than adapted, the scheme operates independently of convergence speed and dispenses with error microphones. The overall structure is depicted in Fig. 2. The SFANC system is divided into a pre-training stage and a control stage.

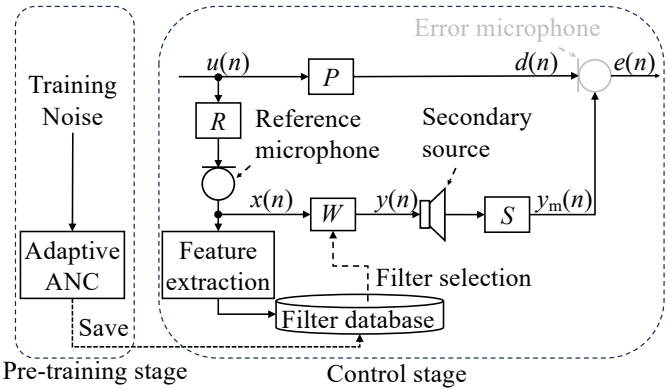

Fig. 2: Block diagram of the selective fixed-filter ANC system.

In the pre-training stage, a suite of band-limited white noise signals is generated, and for each noise scenario an optimal filter is synthesized by means of the conventional FFANC system shown in Fig. 1. The obtained filters are archived in a control-filter database. Subsequently, each noise sample is characterized by its spectral features, and the corresponding optimal filter index serves as a class label. These labelled data are used to train a deep neural classifier.

During the control stage, spectral features are extracted from the incoming reference signal, and the trained classifier selects the most appropriate W from the database. Since no online adaptation is required, the system can achieve rapid noise attenuation without the convergence delays inherent to LMS-type algorithms.

Performance may degrade if the classifier mislabels the noise or if the pre-designed filter set does not adequately span the acoustic conditions encountered in situ. Consequently, attenuation can be sub-optimal in environments that differ markedly from those considered during the pre-training phase. Furthermore, the integration of machine learning and ANC systems increases implementation costs, and machine learning may also lead to incorrect filter selection decisions.

III. Proposed System

To overcome the limitations of the SFANC approach, we propose a selective fixed filter sub-band active noise control system based on reference-signal power estimation. The objective is to choose noise-control filters that match the spectral characteristics of the noise without resorting to machine learning, thereby sustaining high attenuation even under non-stationary noise conditions. The method employs a delayless sub-band ANC framework to design an optimal filter for each frequency band, continually monitors the frequency bands with the highest energy, and switches to the most appropriate filter in real time. The procedure comprises a tuning stage and a

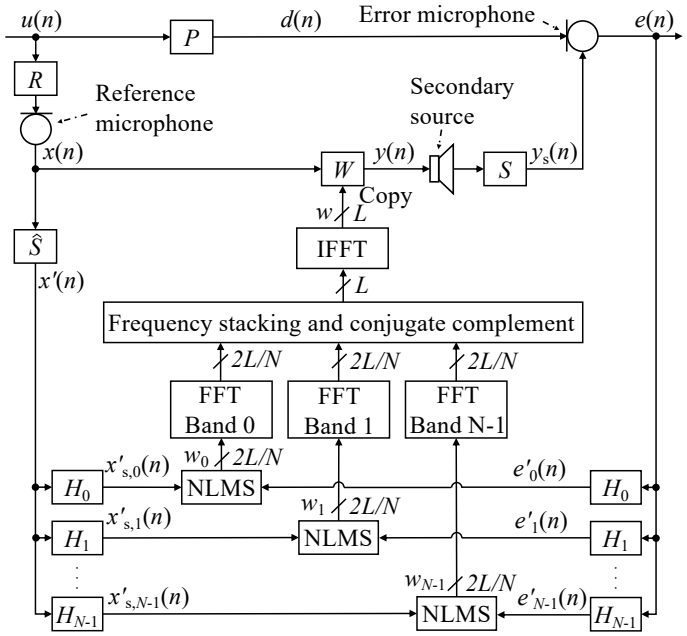

(a) Tuning stage.

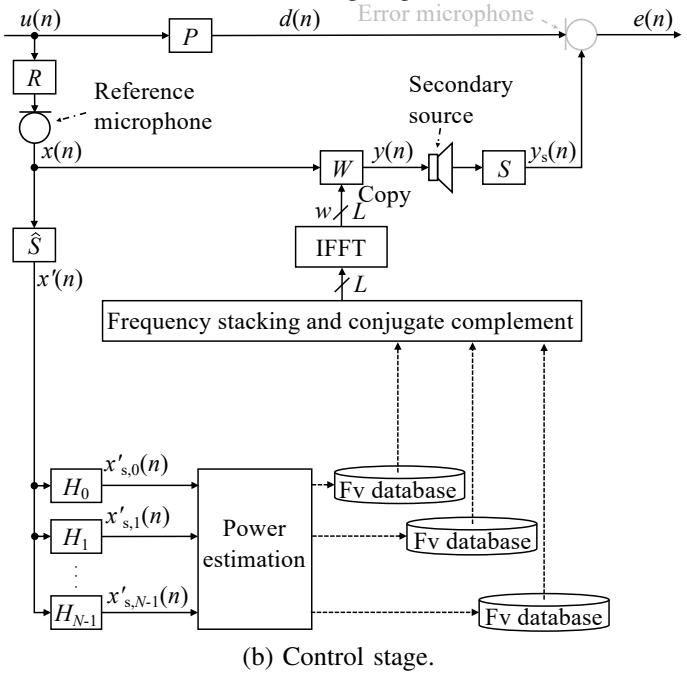

(b) Control stage.

Fig. 3: Block diagram of the proposed ANC system.

control stage.

A. Tuning stage

Fig. 3(a) depicts the tuning stage of the proposed system. An analysis filter bank $H(z)$ decomposes both the filtered reference signal $x'(n)$ and the error signal $e(n)$ into N sub-band components. The m-th sub-band reference signal $x'_{\mathrm{s},m}(n)$ drives an FxNLMS algorithm that updates the sub-band control filter coefficients. The resulting sub-band filters are transformed to the frequency domain via an fast Fourier transform (FFT), recombined by frequency stacking and complex interpolation to reconstruct a full-band response, and finally converted back to the time domain with an inverse FFT (IFFT). The frequency-domain coefficients of the noise control filter obtained without decimation to avoid performance loss at crossover frequencies, are stored in a filter vector database (denoted hereafter as the Fv database).

The analysis filter bank for m-th sub-band $H_m(z)(m = 0, \ldots, N-1)$ is implemented as an N-channel cosine-modulated filter bank derived from a prototype low-pass filter $F(z)$ of length L and cut-off $\pi/2N$:

$$H_i(z) = \alpha_m F\big(zW_{2N}^{m+0.5}\big) + \alpha_m^* F\big(zW_{2N}^{-(m+0.5)}\big), \quad (6)$$

$$\alpha_m = \exp\Big\{j\big[(-1)^m \tfrac{\pi}{4} - \tfrac{\pi}{N}(m+0.5)\tfrac{L-1}{2}\big]\Big\}, \quad (7)$$

where $W_{2N} = e^{-j\pi/N}$ and $(\cdot)^*$ denotes complex conjugation.

B. Control stage

Fig. 3(b) shows the control stage. The filtered reference signal $x'(n)$ is analyzed by the same filter bank $H_m(z)$ to yield sub-band signals $x'_{\mathrm{s},m}(n)$. For each band, the root-mean-square (RMS) power is estimated over a window of B samples:

$$\mathrm{RMS}_{x'_{\mathrm{s},m}}(n) = \sqrt{\frac{1}{B}\sum_{k=n-B+1}^{n} x'^2_{\mathrm{s},m}(k)},$$

$$\mathrm{RMS}_{x'}(n) = \sqrt{\frac{1}{B}\sum_{k=n-B+1}^{n} x'^2(k)}. \quad (8)$$

A sub-band is deemed *active* if

$$20\log_{10}\frac{\mathrm{RMS}_{x_d}(n)}{\mathrm{RMS}_x(n)+\zeta} > \mathrm{Thr}, \quad (9)$$

where $\zeta > 0$ avoids division by zero and Thr [dB] is a user-defined threshold. For each active band, the corresponding filter coefficients are retrieved from the Fv database; inactive bands are zero-padded. The selected sub-band spectra are then stacked, complex-interpolated to a full-band spectrum, converted to the time domain by an IFFT, and copied to the real-time control filter.

The proposed system designs band-specific control filters without machine learning, lowering implementation complexity. Furthermore, because the sub-band spectra are already available, no additional FFT is required during frequency stacking, and the absence of decimation mitigates boundary artifacts.

IV. Evaluations

The effectiveness of the proposed system is evaluated through simulations using impulse responses measured in a real environment.

TABLE I: Design parameters for the frequency-domain coefficients of the noise control filter in the proposed ANC system.

Target noise	White noise (20–8000 Hz)
Sampling frequency	32000 Hz
Update duration	60 s
Number of subbands	32
Prototype filter	Low-pass filter
Analysis filter H	Cosine-modulated filter bank
Control filter tap length	512
Reference path R tap length	150
Primary path P tap length	400
Secondary path S tap length	200
Secondary path model $\hat{S}$ tap length	200
Adaptation algorithm	NLMS
Step-size parameter	4.0×10^{-4}
Normalization coefficient β	1.0×10^{-6}

TABLE II: Simulation conditions.

Controlled frequency range	20–8000 Hz
Sampling frequency	32000 Hz
Number of subbands	32
Prototype filter	Low-pass filter
Analysis filter H	Cosine-modulated filter bank
Power-estimation threshold Thr	-40 dB
Update interval	20 ms
Average sample B	800 samples
Control filter tap length	512
Reference path R tap length	150
Primary path P tap length	400
Secondary path S tap length	200
Secondary path model $\hat{S}$ tap length	200
Step-size parameter	0.01
Normalization coefficient β	1.0×10^{-6}
ζ	1.0×10^{-6}

A. Simulation conditions

Table I summarizes the design parameters for the frequency-domain coefficients of the noise control filter in the proposed ANC system, while Table II lists the conditions employed for the subsequent performance evaluation. The frequency band of the analysis filter $H(z)$ of the proposed ANC system is shown in Fig. 4. The measurement set-up for obtaining the impulse responses is illustrated in Fig. 5; all responses were identified in an anechoic chamber using a real-time digital signal processor (DSP).

In the proposed scheme, a sub-band is deemed active if its power exceeds -40 dB with respect to the broadband reference signal, i.e., $\mathrm{Thr} = -40\,\mathrm{dB}$ in Eq. (9).

Two noise scenarios were examined. Noise 1 (concatenated band-limited noise): a 10-s sequence constructed by concatenating band-limited noise segments with prominent energy in different spectral regions; the dominant band changes abruptly every 1 s. Noise 2 (ESC-50 excerpts): a signal assembled from the ESC-50 dataset [23] in which the noise class (and hence its spectral content) changes every 0.5 s, thereby emulating rapid non-stationary disturbances. The spectrograms of these noises are shown in Fig. 6. Spectrograms were generated using a 1024-point Hamming window with 75 % overlap and a 2048-point FFT.

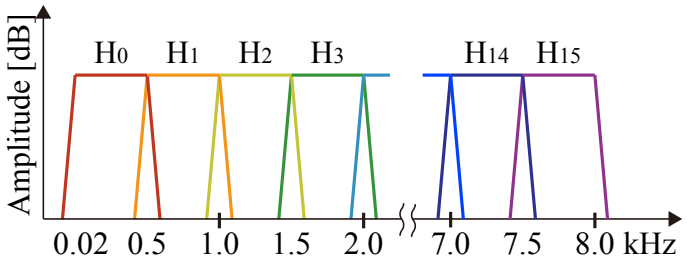

Fig. 4: The frequency band of the analysis filter $H(z)$ of the proposed ANC system.

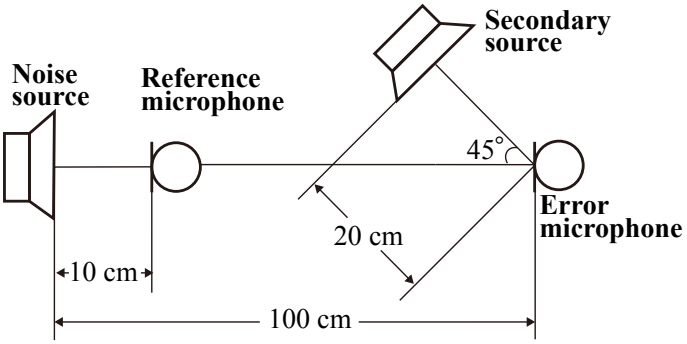

Fig. 5: The measurement set-up.

B. Evaluation of the proposed and conventional systems

Fig. 7(a) shows noise reduction of the proposed and conventional systems for Noise 1. The noise reduction is defined as follows:

$$\mathrm{Reduction}(k) = 10\log_{10}\left[\frac{\sum_{n=1000(k-1)+1}^{1000k} d^2(n)}{\sum_{n=1000(k-1)+1}^{1000k} e^2(n)}\right], \quad (10)$$

where k is the block number.

As can be seen from Fig. 7(a), since the conventional FFANC relies on LMS adaptation, its performance degrades whenever the noise spectrum changes and recovers only after the filter has reconverged. By contrast, the proposed system maintains an attenuation of roughly 25 dB throughout the entire 10-s recording, demonstrating its ability to switch rapidly to a filter matched to the current noise characteristics. A slight dip in performance is observed immediately after each spectral transition; this occurs during the brief interval in which the system selects and loads the new sub-band filter.

Fig. 7(b) shows noise reduction of the proposed and conventional systems for Noise 2, an excerpt from the ESC-50 data set with noise classes changing every 0.5 s. Here, the proposed system still delivers about 20 dB of attenuation, confirming its effectiveness with real-world, non-stationary disturbances. Between 2.0 and 2.5 seconds, however, the conventional FFANC temporarily outperforms the proposed system.

To elucidate this behavior, Fig. 8 plots the spectra the error microphone of the proposed and conventional systems.

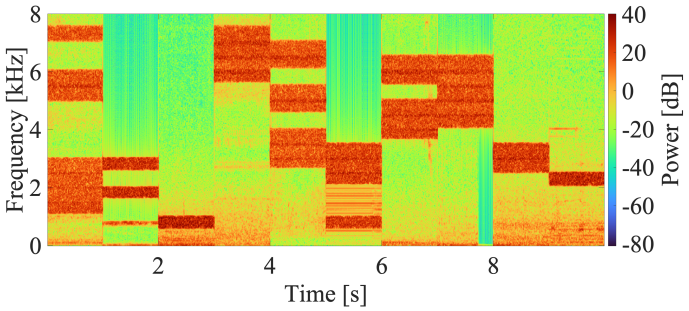

(a) Noise 1

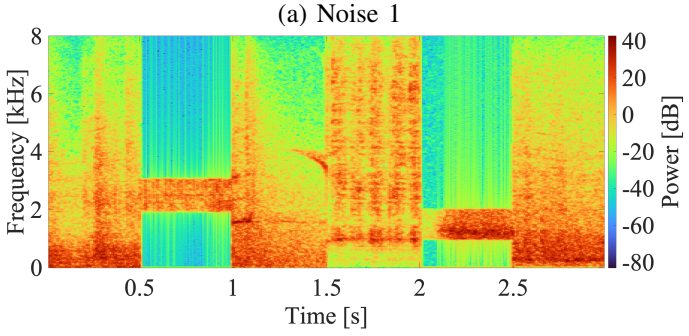

(b) Noise 2

Fig. 6: Spectrogram of noise used for evaluation.

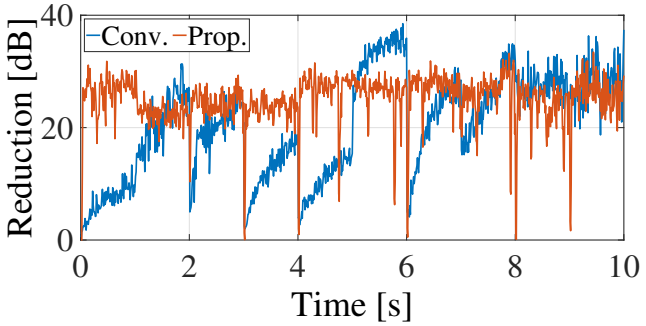

(a) Noise 1

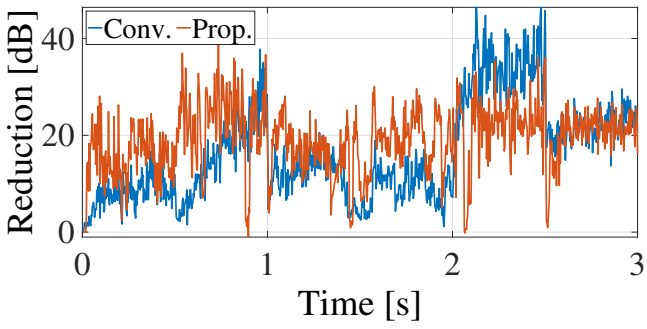

(b) Noise 2

Fig. 7: Noise reduction of the proposed and conventional systems.

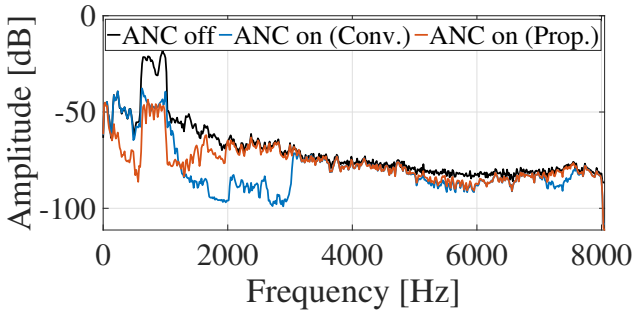

Fig. 8: Spectra at the error microphone of he proposed and conventional systems.

Here, the desired signal when ANC is off is shown in black, and the error signals when the proposed and conventional systems are activated are shown in red and blue, respectively. The frequency spectra were calculated using Welch's method with a Hamming window of 2048 points, 50% overlap, and an FFT length of 2048 points. Both controllers suppress the dominant spectral peaks, but the conventional FFANC achieves approximately 5 dB additional attenuation in the 1-2kHz range. This advantage arises from the continuous adaptation of the conventional system's time-domain filter, which fine-tunes the response within each sub-band. In contrast, the proposed system, which is tuned using white noise and employs 500 Hz-wide sub-bands, does not explicitly target this secondary peak. Nevertheless, the residual energy in the 1-2 kHz range is already below -50 dB, and thus this band is no longer the dominant noise component. At the main peak around 500 Hz, where the disturbance power is highest, both methods achieve comparable attenuation, demonstrating the proposed controller's effectiveness in handling practical noise signals even under rapidly changing conditions.

A limitation of the proposed systems is its sensitivity to non-stationarity of the reference within a sub-band. The sub-band control filters are tuned using white noise, whereas during operation the reference in the k-th sub-band may become spectrally colored, yielding a mismatch and a suboptimal sub-band optimal control filter. This mismatch can be mitigated by increasing the number of sub-bands so that intra-band spectral variation is reduced; however, finer subbanding raises computational cost and can introduce additional distortion in the frequency-stacking stage. Accordingly, the sub-band resolution must be chosen to balance robustness to spectral coloring against reconstruction distortion and complexity.

V. Conclusions

This study proposed the selective fixed filter sub-band ANC system capable of tracking abrupt spectral variations and delivering stable broadband attenuation. During ANC operation, the controller estimates the sub-band power distribution in real time and assembles an instantaneous control filter that is spectrally matched to the prevailing disturbance. Simulation results show that the proposed system sustains more than 20 dB of noise attenuation even under rapidly changing noise conditions. Future work will focus on lowering the computational burden and further enhancing performance by refining the frequency-vector representation in the filter database.

REFERENCES

[1] S. M. Kuo and D. R. Morgan, "Active noise control: a tutorial review," *Proceedings of the IEEE*, vol. 87, no. 6, pp. 943–973, 1999.

[2] S. J. Elliott, *Signal processing for active control*. Academic Press, San Diego, CA, 2001.

[3] Y. Kajikawa, W. S. Gan, and S. M. Kuo, "Recent advances on active noise control: open issues and innovative applications," *APSIPA Transactions on Signal and Information Processing*, vol. 1, p. e3, 2012.

[4] B. Lam, W. S. Gan, D. Shi, M. Nishimura, and S. J. Elliott, "Ten questions concerning active noise control in the built environment," *Building and Environment*, vol. 200, p. 107928, 2021.

[5] S. M. Kuo and D. R. Morgan, *Active noise control systems- Algorithms and DSP Implementations*. New York, NY: John Wiley & Sons, 1996.

[6] F. Yang, J. Guo, and J. Yang, "Stochastic analysis of the filtered-x LMS algorithm for active noise control," *IEEE/ACM Transactions on Audio, Speech, and Language Processing*, vol. 28, pp. 2252–2266, 2020.

[7] M. Ferrer, M. de Diego, and A. Gonzalez, "Filtered-x quasi affine projection algorithm for active noise control networks," *IEEE/ACM Transactions on Audio, Speech, and Language Processing*, vol. 32, pp. 4237–4252, 2024.

[8] W. K. Tseng, "Local active noise control using a novel method of designing quiet zones," *Control Engineering Practice*, vol. 19, no. 12, pp. 1450–1458, 2011.

[9] S. Wrona, M. de Diego, and M. Pawelczyk, "Shaping zones of quiet in a large enclosure generated by an active noise control system," *Control Engineering Practice*, vol. 80, pp. 1–16, 2018.

[10] H. Chen, D. Long, H. Zou, S. Wang, J. Tao, and X. Qiu, "Improving near-field spatial uniformity of secondary sources for active noise control headrests," *Applied Acoustics*, vol. 230, p. 110437, 2025.

[11] X. Shen, D. Shi, W. S. Gan, and S. Peksi, "Adaptive-gain algorithm on the fixed filters applied for active noise control headphone," *Mechanical Systems and Signal Processing*, vol. 169, p. 108641, 2022.

[12] D. Shi, B. Lam, K. Ooi, X. Shen, and W. S. Gan, "Selective fixed-filter active noise control based on convolutional neural network," *Signal Processing*, vol. 190, p. 108317, 2022.

[13] D. Shi, W. S. Gan, B. Lam, and S. Wen, "Feedforward selective fixed-filter active noise control: Algorithm and implementation," *IEEE/ACM Transactions on Audio, Speech, and Language Processing*, vol. 28, pp. 1479–1492, 2020.

[14] D. Shi, W. S. Gan, B. Lam, Z. Luo, and X. Shen, "Transferable latent of CNN-based selective fixed-filter active noise control," *IEEE/ACM Transactions on Audio, Speech, and Language Processing*, vol. 31, pp. 2910–2921, 2023.

[15] Z. Luo, D. Shi, J. Ji, X. Shen, and W. S. Gan, "Real-time implementation and explainable AI analysis of delayless cnn-based selective fixed-filter active noise control," *Mechanical Systems and Signal Processing*, vol. 214, p. 111364, 2024.

[16] X. Su, D. Shi, Z. Zhu, W. S. Gan, and L. Ye, "Spatial-frequency-based selective fixed-filter algorithm for multichannel active noise control," *IEEE Signal Processing Letters*, vol. 31, pp. 2635–2639, 2024.

[17] K. Doi and Y. Kajikawa, "SFANC with compensation filter based on mefxdctlms algorithm," in *2023 Asia Pacific Signal and Information Processing Association Annual Summit and Conference (APSIPA ASC)*, 2023, pp. 1240–1244.

[18] Z. Luo, D. Shi, X. Su, and W. S. Gan, "Frequency-direction aware multichannel selective fixed-filter active noise control based on multi-task learning," *IEEE Transactions on Audio, Speech and Language Processing*, vol. 33, pp. 3137–3147, 2025.

[19] D. Morgan and J. Thi, "A delayless subband adaptive filter architecture," *IEEE Transactions on Signal Processing*, vol. 43, no. 8, pp. 1819–1830, 1995.

[20] S. M. Kuo, R. K. Yenduri, and A. Gupta, "Frequency-domain delayless active sound quality control algorithm," *Journal of Sound and Vibration*, vol. 318, no. 4, pp. 715–724, 2008.

[21] S. Yamanouchi and Y. Kajikawa, "A subband active noise control system with automatic tap assignment in consideration of psychoacoustic properties," in *2021 Asia-Pacific Signal and Information Processing Association Annual Summit and Conference (APSIPA ASC)*, 2021, pp. 1187–1191.

[22] X. Li, C. Lu, W. Chen, Z. Liu, C. Cheng, Y. Wang, and S. Du, "Enhanced selective delayless subband algorithm independent of primary disturbance configuration for multi-channel active noise control system in vehicles," *Mechanical Systems and Signal Processing*, vol. 216, p. 111456, 2024.

[23] K. J. Piczak, "ESC: Dataset for Environmental Sound Classification," in *Proceedings of the 23rd Annual ACM Conference on Multimedia*. ACM Press, pp. 1015–1018.